Using Evoked EMG as a Synthetic Force Sensor of Isometric Electrically Stimulated Muscle

Abbas Erfanian,* Howard Jay Chizeck, *Senior Member, IEEE*, and Reza M. Hashemi

***Abstract*—A method for the estimation of the force generated by electrically stimulated muscle during isometric contraction is developed here. It is based upon measurements of the evoked electromyogram (EMG) [EEMG] signal. Muscle stimulation is provided to the quadriceps muscle of a paralyzed human subject using percutaneous intramuscular electrodes, and EEMG signals are collected using surface electrodes. Through the use of novel signal acquisition and processing techniques, as well as a mathematical model that reflects both the excitation and activation phenomena involved in isometric muscle force generation, accurate prediction of stimulated muscle forces is obtained for large time horizons. This approach yields synthetic muscle force estimates for both unfatigued and fatigued states of the stimulated muscle. In addition, a method is developed that accomplishes automatic recalibration of the model to account for day-to-day changes in pickup electrode mounting as well as other factors contributing to EEMG gain variations. It is demonstrated that the use of the measured EEMG as the input to a predictive model of muscle torque generation is superior to the use of the electrical stimulation signal as the model input. This is because the measured EEMG signal captures all of the neural excitation, whereas stimulation-to-torque models only reflect that portion of the neural excitation that results directly from stimulation. The time-varying properties of the excitation process cannot be captured by existing stimulation-to-torque models, but they are tracked by the EEMG-to-torque models that are developed here. This work represents a promising approach to the real-time estimation of stimulated muscle force in functional neuromuscular stimulation applications.**

***Index Terms*— Artifact suppression, evoked EMG, functional neuromuscular stimulation, muscle fatigue, muscle modeling.**

I. Introduction and Background

FUNCTIONAL neuromuscular stimulation (FNS) can be used to achieve limited restoration of the function of paralyzed muscle. This technology has been used to provide hand grasp to C5–C6 spinal-cord-injured individuals, respiratory pacing for higher level spinal cord injuries, and standing and locomotion for paraplegic and hemiplegic subjects (due to spinal cord injury, stroke, head injury, and other causes), and micturition, bladder, and bowel control. A survey and compilation of the progress in this field is contained in Stein *et al.* [1].

Improved performance of these *neuroprostheses* can, in principle, be obtained through better real-time models of muscle response, either for feed-forward or feedback control. This involves measuring forces, angles, positions, or other appropriate quantities to modify models of the force generation behavior of stimulated muscles. A limiting factor has been the inadequacy of sensors [2], [3]. Sensors for external use are difficult to mount and calibrate, and generally do not directly measure the quantities of interest. In almost all cases, implantable sensors are not available. The use of afferent signals obtained from nerve cuff [4]–[7] or action potentials from peripheral nerves (intrafascicular electrodes [8]) is promising, but significant signal processing problems remain to be resolved.

The standard external methods of measuring muscle force in experimental settings (e.g., see [9] and [10]), which involve motion against fixed test equipment, are not useful for neural prostheses outside of the laboratory. Surgically installed sensors that have been used in animal experiments to characterize muscle properties, such the placement of a force transducer in series with a tendon [11] or the attachment of a buckle transducer to the tendon [12], are not acceptable for rehabilitation in human subjects since they involve damage of the tendon. The introduction of a pressure catheter into the muscle in order to measure the intramuscular pressure [13], has been shown to give good muscle force estimates in the case of voluntary contraction in the unfatigued state. However, this method will probably be confounded by compliance changes in the fascial compartment of the muscle due to different contraction regimes. Also it has not been tested in electrically stimulated muscle. Thus, no adequate muscle force sensors are currently available for deployment in neuroprostheses. This motivates the development of methods to estimate muscle force from quantities that can be measured or well estimated, such as the evoked electromyogram (EMG) [EEMG] and muscle stimulation. *This paper pursues the use of EEMG from stimulated muscle.* The focus of this paper is the development of real time estimates of electrically stimulated muscle output torque from EEMG.

Voluntary and artificial contraction of muscle are accompanied by both electrical and mechanical phenomena, as manifested by electromyogram and force. Over the past four decades, an extensive literature has resulted from investigations of EMG signals arising from voluntary contractions, as a source of information about muscle force, length, or fatigue state. For example, the dynamic relationship between isometric

Manuscript received November 21, 1994; revised July 22, 1997. This work was supported in part by the Iran University of Science and Technology (IUST), by the National Institutes of Health under Grant NS33756, and by the U.S. Department of Veterans Affairs Rehabilitation Research and Development Program (B683). *Asterisk indicates corresponding author.*

*A. Erfanian is with the Department of Biomedical Engineering, Iran University of Science and Technology, Narmak, Tehran 16844 Iran (e-mail: erfanian@rose.ipm.ac.ir).

H. J. Chizeck is with the Department of Systems, Control, and Industrial Engineering, Case Western Reserve University, Cleveland, OH 44106-7070 USA.

R. M. Hashemi is with the Amirkabir University of Technology, Tehran 15914 Iran.

Publisher Item Identifier S 0018-9294(98)00909-4.

tension and the electromyogram is described by a second-order linear system [14]. In [15], this relationship is characterized by Hill-based model, where the smoothed rectified EMG and joint angle are the inputs of the model and the output is force. In [16], this filtered EMG signal is used to estimate ankle and knee moments during walking.

The characterization of the relationship between EEMG and muscle torque in electrically stimulated muscle has not been extensively studied. In [17] it was shown that there exists a nearly linear relationship between the mean-absolute value (MAV) of EEMG and isometric force, when cat muscle is stimulated via cuff electrodes and EEMG is recorded by intramuscular electrodes (for a specific stimulation pattern). Other studies in the literature reported changes in the MAV of the EEMG that appear to be associated with isometric force changes, but do not describe functional relationships between these variables [18], [19].

Although a large number of mathematical models of electrically stimulated muscle have appeared (as reviewed in [23]), these efforts have not resulted in predictive models of muscle force that can be used for real-time control in neuroprostheses. *There is no available model that accurately predicts muscle force on the basis of EEMG.* Models that predict muscle force from stimulation information [10], [11], [24] do well for short prediction time intervals, but exhibit normalized output prediction errors of 15% or greater for prediction of times that are more than 0.5 s in the future [10], even when they are allowed to generate time-varying parameter estimates. Although such identified models can be useful in adaptive controllers [25], [26], they are not accurate enough for the careful coordinated control of groups of muscles in multijoint systems.

In this paper, we develop a method for estimating the torque generated by electrically stimulated muscle during isometric contraction based upon measurements of the EEMG. Muscle stimulation is provided to the quadriceps muscle of paralyzed human subjects using percutaneous intramuscular electrodes, and EEMG signals are collected using differently mounted surface electrodes. Through the use of appropriate signal acquisition and processing techniques, as well as a mathematical model that reflects both the excitation and activation phenomena involved in isometric muscle force generation, we can obtain accurate prediction of stimulated muscle torque for large time horizons. For muscle that is not fatigued, this approach yields synthetic muscle torque estimates for any stimulation pattern. For fatigued muscle, it provides excellent torque estimates if the muscle is either maximally stimulated, or submaximally stimulated by a cyclically repeating pattern.

A. Experimental Procedure

Experiments were conducted on two complete-level-T7 spinal cord injury paraplegics (six years and 18 years post injury). The subjects were active participants in a rehabilitation research program involving daily electrically stimulated exercise of their lower limbs (either seated or during standing and walking), as described in [27]. Percutaneous intramuscular electrodes were implanted near the motor points of the major lower limbs as described in [28]. During the experiments reported here, only the lower limb vastus lateralis muscle was stimulated, by activating merely the corresponding intramuscular electrode. The muscle was stimulated using pulse-width modulation at a constant frequency (20 Hz) and constant amplitude (10 mA), under isometric conditions. The knee of the test leg was fixed securely in 30° of flexion (where full extension is 0°).

Isometric knee torque was measured using a Cybex II dynamometer. The subject was seated on the bench of Cybex machine, with his hip flexed at approximately 90° and his thigh held against the seat with a restraining strap. An instrumented torque arm (having a set of strain gauges) was used to measure the isometric muscle torque. Calibration of the sensors was done to remove the effects of passive torque and loading. Measured values of the knee torque were lowpass filtered (cutoff frequency 100 Hz), and sampled at 1200 Hz. The sampled values were then subdivided into blocks with each block containing 60 data points (i.e., the number of data points over each period of stimulation). The measurements within each block were then averaged. EEMG data were collected by a differential amplifier with a common mode rejection ratio of 120 dB and bandwidth of 250 kHz, and then sampled at a rate of 1200 Hz.

Stimulation Input Patterns: The choice of stimulation input pattern can affect the identification of parametric models of electrically stimulated muscle, since persistent excitation is required for identification algorithm convergence [29]. We used six types of input patterns in this study. Two stochastic patterns were used for dynamic model parameter identification. They were chosen to guarantee persistent excitation.

The first pattern consisted of a succession of 1-s-long sets of 20 pulses, where the first ten pulsewidths were increased from a fixed minimum value to a randomly determined maximum value, and then the next ten pulses symmetrically decreased. The maximum pulse width (for the tenth pulse in each set) was randomly chosen to vary between 0 and 25 μs, according to a uniform distribution.

In the second stimulation pattern, sets of ten pulses were delivered, where these pulses monotonically increased or decreased in pulse width. Both the initial and final pulse width values were randomly selected (uniformly distributed between 0 and 25 μs). The increment between each successive pulse width was the same in this second stimulation pattern.

The third type of stimulation pattern consisted of a 2.5-s sequence of constant pulsewidths. The fourth type of stimulation pattern was a 2.5-s sequence of monotonically increasing pulsewidths. These two stimulation patterns were used to study the transient dynamics and recruitment characteristics of the electrically stimulated muscle.

Finally, two stimulation patterns were used for investigation of potentiation and fatigue processes. The fifth type of stimulation pattern was a 5-min sequence consisting of a periodic ramp-and-hold signal (period $=$ 25 s). The sixth type of stimulation pattern consisted of a 5-min-long sequence of constant pulsewidths. Figs. 1, 8, and 9 illustrate examples of these input stimulation patterns.

II. Artifact Suppression

The recording and processing of the EEMG in electrically stimulated muscle present technical difficulties, due to the need

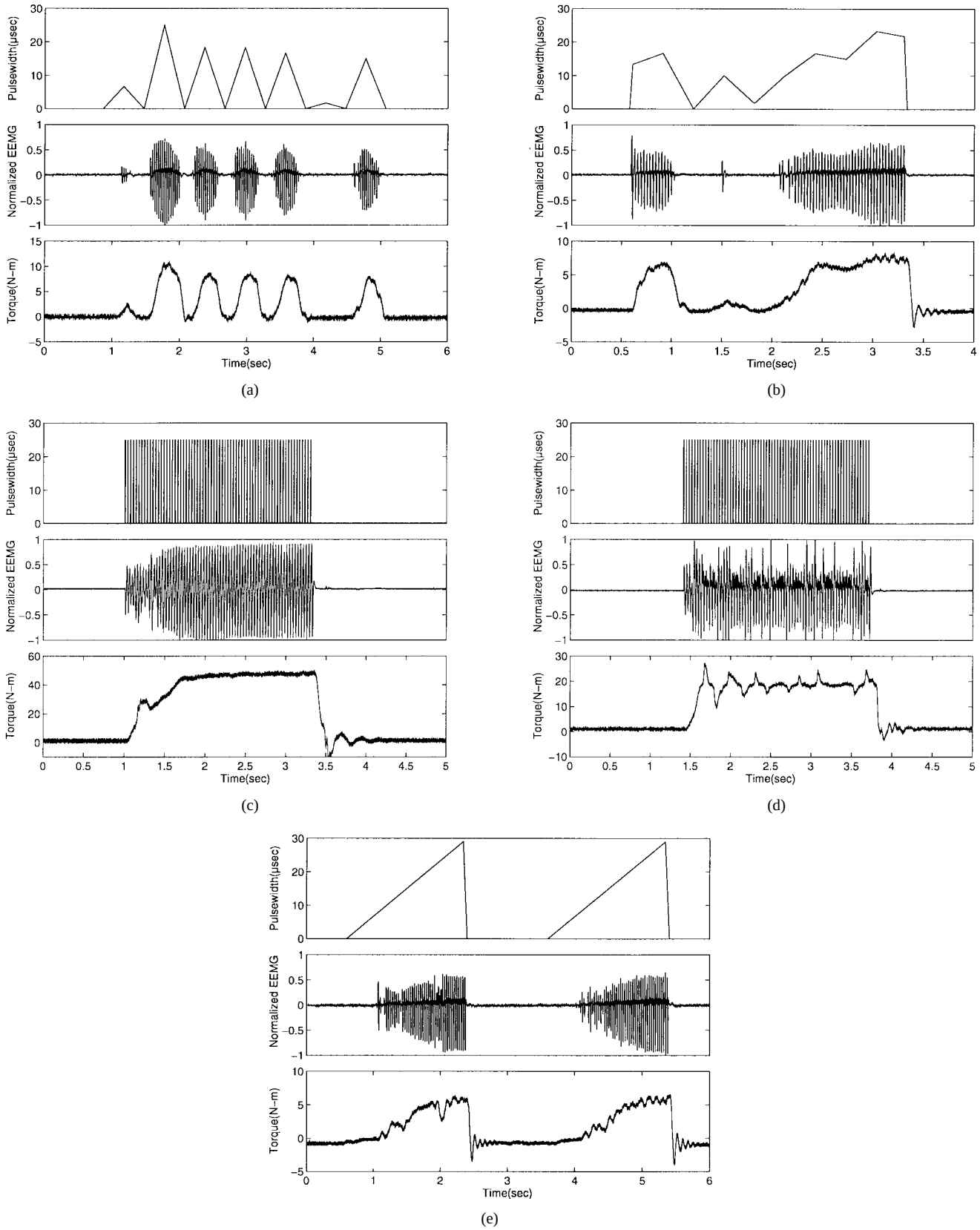

Fig. 1. Typical examples of the stimulation patterns: (a) first type; (b) second type; (c) third type, consisting of a 2.5-s sequence of constant pulsewidths; (d) another example of the third type; and (e) fourth type, consisting of two 2.5-s sequences of monotonically increasing pulsewidths.

to suppress the stimulus artifact. The stimulus artifact results from the potential difference between the EEMG recording electrodes. This potential is produced by the electric field of the stimulus current source. The shape of stimulus artifact depends upon the shape of stimulus pulse, the source-field distance, the amount and type of tissue between the stimulus

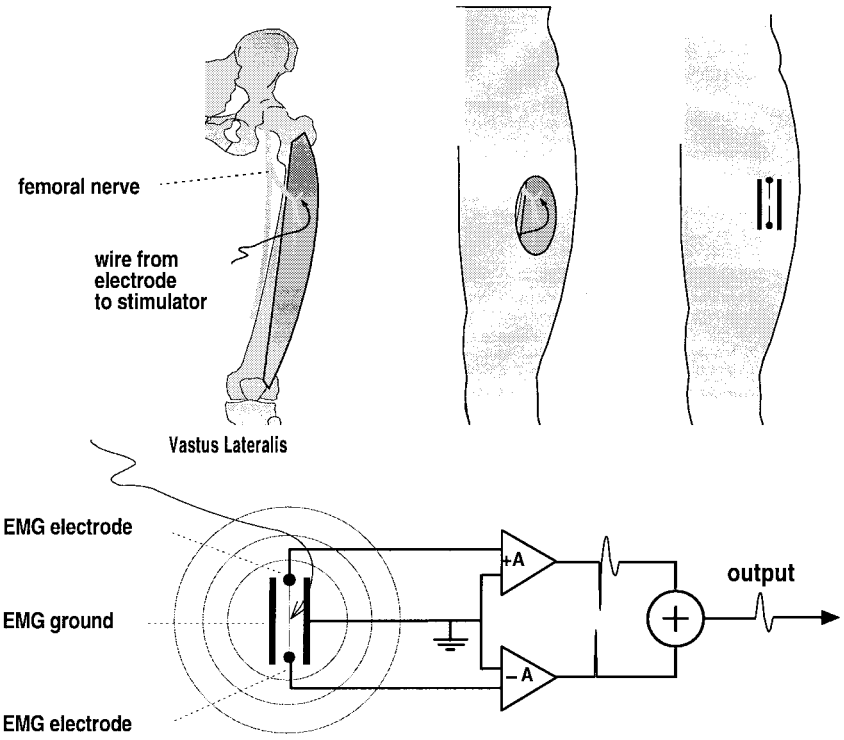

Fig. 2. Illustration of the EEMG recording procedure. The recording electrodes are placed on the skin surface symmetrically, with respect to the point current source inside of the body. This symmetric placement reduces the stimulus artifact. In addition the induced electric field of the point current source is dampened by a pair of patch ground electrodes, which are put on the skin parallel to the recording electrodes. The interelectrode spacing is 3 cm with 5-mm-diameter EMG electrodes.

source and recording electrode sites, as well as the orientation of recording electrodes.

Several different methods for the elimination of stimulus artifacts appear in the literature. In [20], for cat muscles stimulated by nerve cuff electrodes and EEMG recorded by intramuscular electrodes inserted in the belly of the muscle, the stimulus artifact was suppressed by a lowpass Chebyshev filter. When this method is used, the EEMG may be distorted by low frequency components of the stimulus artifact.

Several methods of stimulus artifact suppression through the use of signal blanking circuitry have been proposed. For example, in [21] the stimulus artifact produced by a surface voltage source stimulator was suppressed using a dead-zone blanking circuit in cascade with a lowpass filter. In [22] artifact suppression was attained for a current source surface stimulator, based on switching the input of a dc amplifier to earth during the stimulus pulses. In [32] a system was proposed for suppression of the stimulus artifact, based upon the use of a surface hybrid (voltage and current source) stimulator, in combination with a slew rate limiter, and signal blanking. The output of hybrid stimulator switched from current source during pulses to voltage source in between pulses, in order to shorten artifact transients. The actual artifact suppression was accomplished by the slew rate limiter and signal blanking circuitry.

A difficulty in the use of this type of approach is the need to correctly set the timing of the circuitry for the artifact suppression. Determination of the settings depends strongly on the shape, frequency and width of the stimulation pulses, as well as on the time delay between the stimulus and the artifact. For pulse-width modulation involving long pulses or short distances between the recording site and stimulation source, the artifact and EEMG overlap. In this case, the above methods do not work, because a part of the EEMG signal is itself suppressed. For stimulus-period modulation, the timing of the artifact suppression circuitry must be changed simultaneously with changes in the frequency of stimulation.

In this work, we have developed a recording technique for overcoming the stimulus artifact when the muscle was stimulated by an intramuscular electrode. EEMG measurements were acquired using two surface electrodes placed on the skin, parallel to the long axis of the muscle, over the bulk of the vastus lateralis. The skin directly under the surface electrodes was cleaned by alcohol, in order to reduce the impedance between the recording surfaces and the signal sources. In order to avoid electrode movement and loose contacts, the electrodes were secured to the skin with adhesive tape. By careful placement of these electrodes and the EEMG ground electrode, and through the use of differential signal processing methods, the stimulation artifact was removed and a single EEMG signal was obtained. These procedures, which we call *artifact balancing*, are described below.

Artifact Balancing: There are three principal procedural concerns involved in this approach. They are the following.

1) Positioning of the surface electrodes.
2) Selection of pick-up electrode size and interelectrode spacing (a bandwidth issue).
3) Placement of patch-ground electrodes.

The principle of this method is as follows: Let Φ_A and Φ_B be the induced electric potentials of the points A and B on the

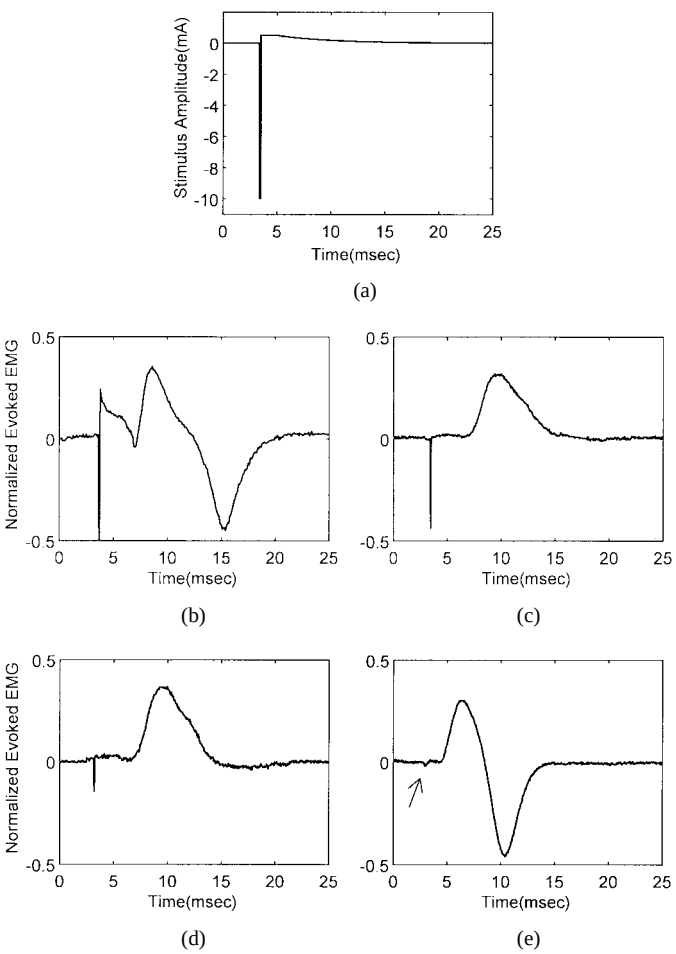

Fig. 3. (a) Pulse shape of the stimulation signal. (b) Measured EEMG when one recording electrode is placed over the bulk of the lower-limb vastus lateralis muscle and the other over the most distal portion of the muscle. (c) and (d) EEMG obtained with a 3-cm interelectrode spacing and a single ground between them. (e) EEMG obtained with the artifact balancing procedure.

body surface due to the point source of a current stimulator inside the body. Then the stimulus artifact voltage is given by

$$V_{artifact} = \Phi_A(\overline{r}_A) - \Phi_B(\overline{r}_B).$$

Positioning: Here, $\overline{r}_A$and $\overline{r}_B$ are source-field distances. If the source-field distances $\overline{r}_A$and $\overline{r}_B$ are equal, then we would expect that the electric potentials Φ_A and Φ_B would be almost the same, and the stimulus artifact would be extremely small. Since the stimulation electrode is implanted near the muscle motor point, careful placement of the recording electrodes on the muscle surface can achieve this equivalence of source-field distances. If the distance between the recording electrodes is small, then the source-field distances $\overline{r}_A$and $\overline{r}_B$ are approximately equal and consequently $\Phi_A \approx \Phi_B$. That is, the artifacts are balanced and, thus, cancel each other. However, reducing the interelectrode spacing is limited by the wavelengths of the muscle-fiber action potentials, by the lowpass-filtering properties of the intervening tissue and by the lowpass-filtering properties of the electrodes themselves.

Size: Larger electrodes provide higher signal-to-noise ratios (SNR's) and lower cutoff frequencies than smaller electrodes [30]. Selection of the diameter of the pick-up electrodes involves a compromise between the desired SNR and the desired bandwidth.

Placement: We damp the induced electric field of the point current source with a pair of patch-ground electrodes which are put on the skin, parallel to the recording electrodes. A diagram illustrating this EEMG recording procedure is shown in Fig. 2.

Results of Artifact Suppression: In order to illustrate that this artifact suppression method works, we first sample the EEMG at 20 kHz. Fig. 3(b) shows the EEMG obtained when one electrode was placed over the bulk of the lower limb vastus lateralis muscle and the other over the most distal portion of the muscle. Fig. 3(c) and (d) shows the EEMG with a 3-cm interelectrode spacing and a single ground between them. The improvement seen in Fig. 3(d) is due to better pick-up electrode placement. The results presented in Fig. 3(e) demonstrate the stimulus artifact reduction obtained by the symmetric placement of the EEMG electrodes, with respect to the stimulating electrode (and with symmetric placement of the grounds). A 3-cm interelectrode spacing and 5-mm diameter EMG electrodes were used, in the configuration shown in Fig. 3.

Fig. 1(a) shows the processed measurements obtained when the first type of stochastic input stimulation pattern is used. The Cybex torque measurements have been processed as described earlier, and the EEMG was obtained using the artifact-balancing method. Fig. 1(b) illustrates the analogous data when the second type of stochastic input pattern is used. Fig. 1(c) and (d) shows the EEMG and torque generated by a sequence of constant width pulses. Note that the torque and the EEMG rise times track each other quite well. However, due to the properties of the mechanical load, the passive mechanical properties of muscle and muscle latency, torque continues to be generated after the EEMG ceases. Fig. 1(d) is quite revealing, in that the "ragged" torque response closely matches changes in the EEMG. Fig. 1(e) shows ramp responses. Note that although the same input pattern is repeated, both the EEMG and the torque signals show considerable variation. However, as will be discussed later, the EEMG and torque signals are highly correlated. These figures suggest that the measurements of the EEMG might be used to predict the torque. This conjecture is investigated in Section III.

III. Identification of Muscle Torque Models

We can use the torque measurements, information about the stimulation signal and the EEMG measurements (as obtained using the methods described above) to identify the parameters of mathematical models of muscle torque production. Three types of models are considered here 1) *contraction dynamics model*, relating the EEMG to measured torque (EEMG-to-torque model); 2) *excitation dynamics model*, relating the stimulation to the measured EEMG (stimulation-to-EEMG model), 3) *overall muscle dynamics model*, relating stimulation to the torque that is generated (stimulation-to-torque model). Fig. 4 schematically illustrates these three situations. Note that muscle contraction is the result of neural excitation due to stimulation signal as well as from other sources, such as reflex

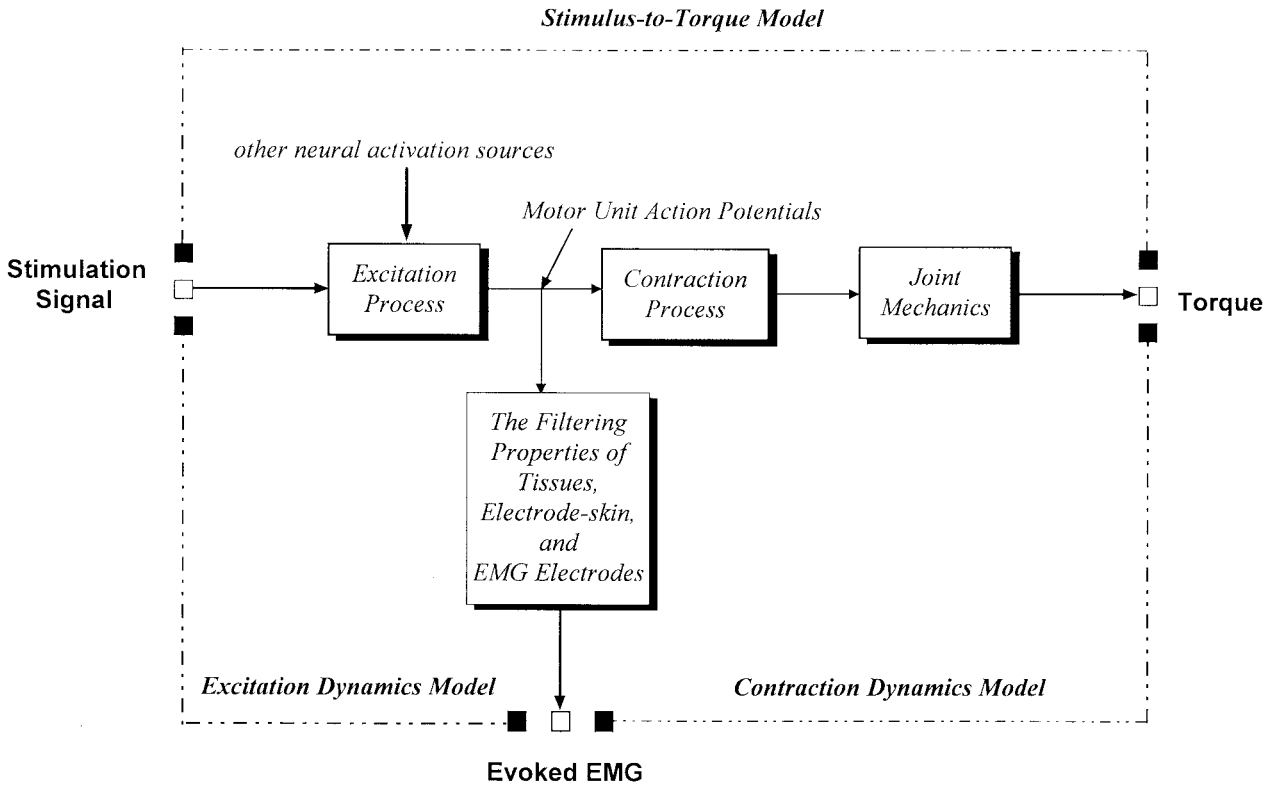

Fig. 4. Diagram illustrating the modeling factors considered in this work; the *contraction dynamics model*, relating the measured EEMG to measured torque; the *excitation dynamics model*, relating the stimulation to the measured EEMG; and the *overall muscle dynamics model*, relating the stimulation to the resulting torque.

and spasticity. The measured EEMG reflects this combination, filtered by the electrical properties of tissue and the pick-up electrodes. Of course any change in the location of the stimulus electrode may cause the level of activation to change.

The literature regarding identification of models of electrically stimulated muscle is quite large (e.g., see [1], [10], [11], [24]). The innovation in this work is the explicit consideration of both the excitation and the contraction dynamics.

Contraction Dynamics Model: To capture the contraction dynamics, a Hammerstein model was used. This consists of two subsystems in cascade. The first subsystem is a memoryless nonlinearity (approximated by a polynomial). The second subsystem is a linear dynamic system. This approach has been used for identification of the muscle dynamics, including the recruitment nonlinearity of intramuscular electrodes, when the model input is the stimulation [10]. In this work, we apply it when the model input is *the mean-absolute value* (MAV) of the EEMG.

The linear part of the Hammerstein model is chosen to be a deterministic autoregressive moving average (DARMA) model, which can be described in operator notation [29] as

$$y(t) = A(q^{-1})y(t) + B(q^{-1})u(t) \tag{1}$$

where

$$\begin{aligned} A(q^{-1}) &= a_1 q^{-1} + a_2 q^{-2} + \cdots + a_l q^{-l} \\ B(q^{-1}) &= b_1 q^{-1} + b_2 q^{-2} + \cdots + b_m q^{-m}. \end{aligned} \tag{2}$$

Here, $y(t)$ is the muscle output torque at time t, $u(t)$ is the activation level of the muscle at time t, and $q^{-1}$is the backward shift operator. The activation level is modeled as an nth-order polynomial function of the instantaneous EEMG signal, $x(t)$, by

$$u(t-i) = \sum_{j=1}^{n} \gamma_{ij}[x(t-i)]^j \qquad i = 1, 2, \cdots, m. \tag{3}$$

Substituting (2) and (3) into (1) and expanding

$$y(t) = \sum_{i=1}^{l} a_i y(t-i) + \sum_{i=1}^{m}\sum_{j=1}^{n} \mu_{ij}[x(t-i)]^j + a_0 \tag{4}$$

where

$$\mu_{ij} = b_i \gamma_{ij}.$$

Measured values of the muscle torque and the MAV of the EEMG are used to fit parameters of model (4). The a_0 term is used to fit any offset in the output (that is, a nonzero output corresponding to a zero EEMG input). In this application, due to the deadband associated with the EEMG pickup and amplification, such an offset can occur.

Identification of the Model: A key stage of identification of the unknown parameters (a_j, μ_{ij}) is selection of the model-order parameters (l, m). In this work, different choices of the model-order parameters were assumed, and then the resulting model was identified [that is, values of the (a_j, μ_{ij}) were fit from measured torque and measured EEMG data]. Standard weighted recursive least-squares (RLS) methods were used to fit these parameters [29].

During each experiment day, 30 trials were conducted. In these trials, the second type of stimulation input pattern

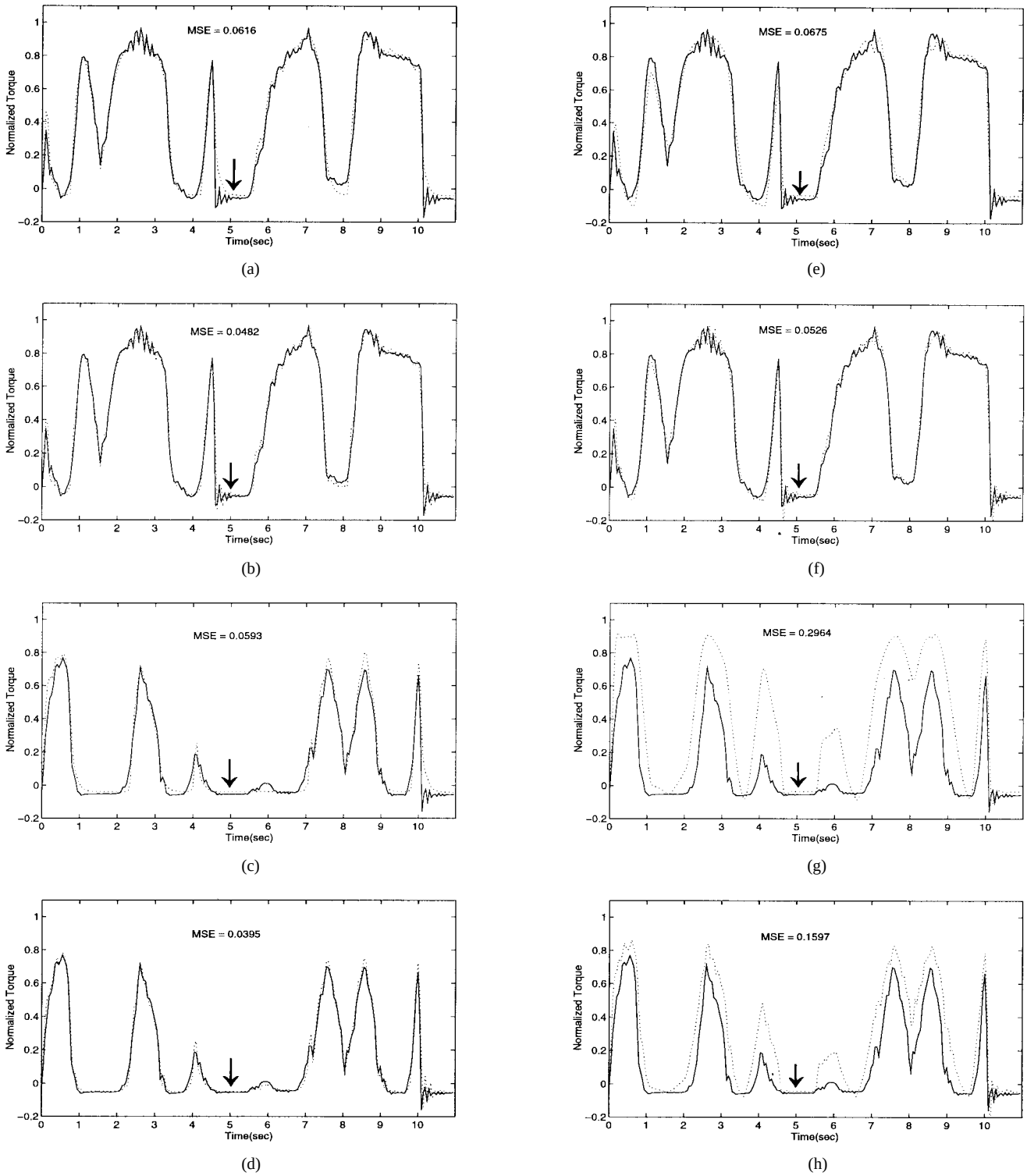

Fig. 5. (a) The measured (solid line) and predicted (dotted line) torque obtained using the *muscle contraction dynamics model*. The prediction is based on the measured EEMG and past predicted torque [$\hat{y}_p(t)$], for two successive trials of the five trials that provided data for model fitting. The markers within the figures indicate the end of the one trial, and the beginning of the next; (b) the same information as in (a) when prediction is based on the measured EEMG and past measured torque [$\hat{y}_m(t)$]; (c) and (d) the measured and predicted torque when the predictors $\hat{y}_p(t)$ and $\hat{y}_m(t)$ are used, respectively, for data obtained in two trials that were not used to fit the model; (e)–(h) the same information as in (a)–(d) when the stimulation-to-torque model is used.

(described in Section I) was used. There were three separate experiment days, each following the same sequence of trials. Model parameters were identified for each day. One concern in using recursive methods to identify these parameters is the need to have a long enough run of successive inputs (and their corresponding outputs). In this work, the duration of each trial was 5 s. Thus, 100 points were available, per variable, in each trial. Each trial began and ended with an interval of no stimulation. Thus, if desired, data from successive trials (or other different trials) could be concatenated for purposes of

TABLE I
SUMMARY OF THE AVERAGE DAILY PREDICTION ERROR (150 s) OBTAINED FOR BOTH THE CONTRACTION DYNAMICS MODEL (EEMG-TO-TORQUE) AND THE OVERALL DYNAMICS MODEL (STIMULUS-TO-TORQUE)

	Subject	Day 1		Day 2		Day 3	
mean-squared torque prediction error		$\hat{e}_m$	$\hat{e}_p$	$\hat{e}_m$	$\hat{e}_p$	$\hat{e}_m$	$\hat{e}_p$
EMG-to-torque model	EB	0.0427	0.0612	0.0443	0.0850	0.0454	0.0754
	DN	0.0207	0.0284	0.0185	0.0282	0.0259	0.0431
stimulus-to-torque model	EB	0.1238	0.2262	0.0497	0.1154	0.1383	0.2951
	DN	0.0298	0.0567	0.0269	0.0558	0.0363	0.0821

Note that on each day, the identified contraction dynamics model provides better predictions of the output torque than the overall model. Here $\hat{e}_m$ and $\hat{e}_p$ are the mean-square prediction errors based on the predictor $\hat{y}_m(t)$ or $\hat{y}_p(t)$, respectively. The predictor $\hat{y}_m(t)$ is based on the input (stimulation for overall model and measured EEMG for contraction model) and the past predicted measured. The predictor $\hat{y}_p(t)$ is based on the input (stimulation for overall model and measured EEMG for contraction model) and the past predicted torque.

TABLE II
SUMMARY OF THE AVERAGE DAILY PREDICTION ERROR (70 s) OBTAINED FOR BOTH THE EXCITATION DYNAMICS MODEL (STIMULUS-TO-EEMG) AND THE CONTRACTION DYNAMICS MODEL (EEMG-TO-TORQUE)

	Subject	Day 1	Day 2	Day 3	Day 4	Day 5	Average
Steady State Gain (computed from identified excitation model)	EB	0.3435	0.5770	0.5966	0.8791	0.5051	
	DN	0.3420	0.3226	0.3196	0.3109	0.2004	
Mean Squared EMG Prediction Error (using EMG predictor $\hat{x}_m(t)$)	EB	0.0367	0.0559	0.0643	0.0408	0.0717	0.0538
	DN	0.0510	0.0417	0.0462	0.0586	0.0404	0.0476
Mean Squared EMG Prediction Error (using EMG predictor $\hat{x}_p(t)$)	EB	0.0417	0.0595	0.1124	0.0446	0.0751	0.0666
	DN	0.0582	0.0477	0.0516	0.0594	0.0427	0.0519
Mean Squared Torque Prediction Error(using EMG predictor $\hat{x}_p(t)$ and Torque predictor $\hat{y}_p(t)$	EB	0.0644	0.0548	0.1276	0.0397	0.0802	0.0733
	DN	0.0532	0.0542	0.0496	0.0601	0.0466	0.0527
Mean Squared Torque Prediction Error (using past measured EMG and Torque predictor $\hat{y}_p(t)$)	EB	0.0504	0.0413	0.0852	0.0343	0.0464	0.0515
	DN	0.0249	0.0381	0.0235	0.0423	0.0256	0.0309

identification. In order to limit fatigue, a resting period of 1 min was enforced between each 5-s trial.

We chose to represent the recruitment curve of muscle as a third-order polynomial, ($n = 3$), as in [10]. Model-order determination was accomplished by comparing the Akaike's final predication-error criterion (FPEC) [29] obtained, for different model orders. Model-order parameters ranging from $2 \leq m \leq 8$, and from $2 \leq l \leq 8$ were considered. We found that the FPEC was minimized by model order ($m = 2$, $l = 3$). The same values were obtained for all three days. The FPEC was used, rather than the more common Akaike's information-theoretic criterion, because no information about the underlying distribution of stochastic process was assumed. The FPEC provides a combined measure of fitting error and over-parameterization.

Model Validation: The credibility of the identified model can be determined by its ability to predict the outputs that result from *different* inputs. For a muscle response model, an additional consideration in determining the appropriateness of the model is its ability to predict muscle torque under a variety of conditions. We use the *mean-square error* (MSE) as a performance index for measuring the quality of prediction, as follows:

$$\text{MSE} = \left[\frac{1}{T}\sum_{t=0}^{T}[y(t) - \hat{y}(t)]^2\right]^{1/2}$$

where $y(t)$ is the output muscle force at time t, and $\hat{y}(t)$ is the model output based on the identified parameters. There are two possible versions of $\hat{y}(t)$ that can be used in this measure. One approach is to compute $\hat{y}(t)$ as a function $\boldsymbol{f}$ of past *measured* values of the muscle output and measured EEMG

$$\hat{y}_m(t) = f[x(t-1), x(t-2), \cdots, x(t-m) \\ y(t-1), y(t-2), \cdots, y(t-l)].$$

This might be called "one step ahead" prediction. The second approach is to compute $\hat{y}(t)$ as a function of measured EEMG and past *predicted* values of the muscle output

$$\hat{y}_p(t) = f[x(t-1), x(t-2), \cdots, x(t-m), \hat{y}_p(t-1), \\ \hat{y}_p(t-2), \cdots, \hat{y}_p(t-l)].$$

The use of the first approach begs the issue of model validation, since the prediction capability of the identified model is not tested (instead, measured y values are used). The second approach explicitly captures identified model performance, since it explicitly uses predicted output values. However, for model-order determination, the one-step method is preferred, since we avoid correlation with past predictions. From practical point of view, the one-step ahead prediction is irrelevant, because the torque measurements are not available. There are two versions of mean-square prediction error, depending upon which version of $\hat{y}(t)$ is used; $\hat{e}_m$ is based on $\hat{y}_m(t)$; $\hat{e}_p$ is based on $\hat{y}_p(t)$.

We concatenated data from five successive trials, in order to identify the complete set of model parameters. The resulting

identified model was then validated using the data collected from the other 25 trials conducted on that experiment day.

Fig. 5(a) shows the measured and predicted torque, obtained using the $\hat{y}_p(t)$, for two successive trials, of the five trials that provided the data for model fitting. The markers within the figures indicate the end of the one trial, and the beginning of the next. Fig. 5(b) shows the same information when the predictor $\hat{y}_m(t)$ is used. In both cases, good fits are obtained (6% and 5% normalized MSE, respectively). Fig. 5(c) and (d) shows the corresponding fits when this model is used for two of the other trials on the same experiment day (i.e., not with the same data that was used for the model identification). Once again, good fits are obtained. Note that the two predictor types achieve approximately the same amount of fitting error. As expected, the fit obtained using additional measurements is better. Similar results were obtained on the other two experiment days.

Overall Muscle Dynamics Model: We next consider identification of a model relating the input stimulation signal to the measured muscle torque. This was done using data collected from the 90 trials described above. Using the stimulation pulsewidths as the input values, different order Hammerstein models were fit. In all cases, the polynomial order was assumed to be three. Based on FPEC, the other model orders were determined to be ($m = 2$, $l = 2$). It was observed that using $l = 3$ yielded the same FPEC. For model simplicity, the lower order was chosen, as in our prior work [24].

The overall muscle dynamics model was identified using the data collected from the five successive trials. The resulting identified model was then validated using both information updating schemes [i.e., $\hat{y}_p(t)$ and $\hat{y}_m(t)$]. That is, torque prediction is based on the stimulation signal and past measured values of the muscle output, when using $\hat{y}_m(t)$, or past predicted values of the muscle output, when using $\hat{y}_p(t)$. Fig. 5(e) and (f) illustrates the measured and predicted torque outputs obtained during the same 5-s intervals as in Fig. 5(a) and (b), using both predictor approaches but fitting an overall muscle dynamics model. As before, both update approaches yield good predictions, but the predictions that are obtained using the additional measurements in $\hat{y}_m(t)$ are somewhat better. Fig. 5(g) and (h) shows the measured and predicted torque that are obtained using this model, for data obtained in two 5-s trials that were not used to fit the model [the same trials as in Fig. 5(c) and (d)]. Comparing these figures, we see that the EEMG-to-torque model is far more accurate than the stimulation-to-torque model, particularly when torque measurement values are not available.

Table I summarizes the average daily prediction errors obtained for both the contraction dynamics model (measured EEMG-to-torque) and the overall model (stimulus-to-torque), for both subjects. On each day, the identified contraction dynamics model (measured EEMG-to-torque) provides better predictions of the output torque than the overall model (stimulation-to-torque). A possible explanation for this difference is that the measured EEMG signal reflects the total neural input to the muscle. The EEMG includes components that are not present in the stimulation signals. The stimulation-to-torque model cannot capture the effects of these other, nonevoked EMG signals (reflecting spasticity or activation of motoneurons due to reflex phenomena). It also cannot capture changes in the recruitment properties of the stimulating electrode, due to changes in muscle geometry that are induced by contractions (or other time variations in the recruitment characteristic). The predictive capability of the stimulation-to-torque model is also damaged by any changes in the excitation gain (from stimulation to EEMG) that might occur. For example, changes in the stimulation electrode ground may provide a source of variability which degrades the stimulation-to-torque model predictions, but not the measured EEMG-to-torque model.

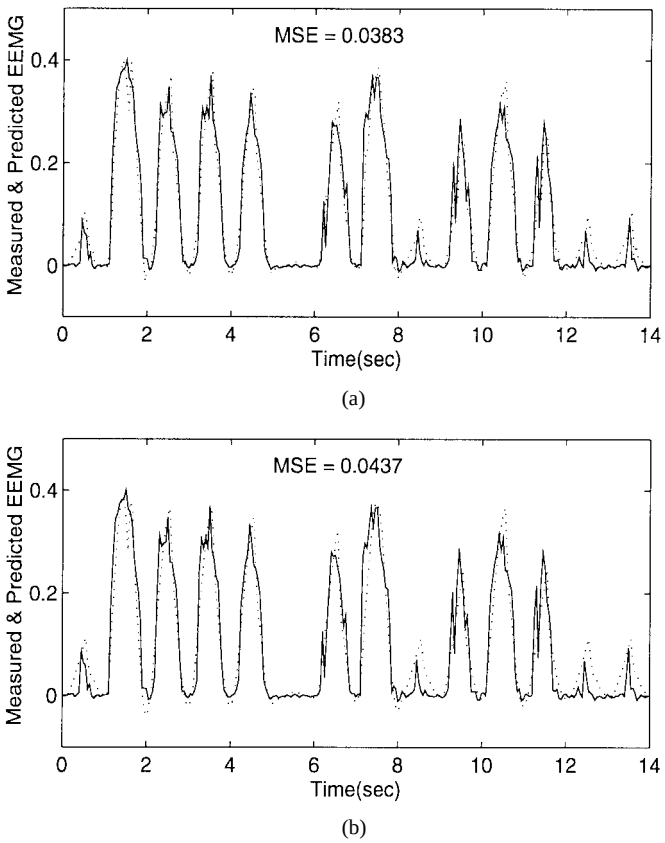

Fig. 6. The measured (solid line) and predicted (dotted line) MAV of the EEMG obtained using *muscle excitation dynamics model* for two successive trials on the same day: (a) when prediction is based on the stimulation signal and past measured EEMG; (b) when prediction is based on both the stimulation signal and past predicted EEMG.

IV. Identification of the Excitation System

It is possible to fit parameters to model of the excitation process (i.e., from stimulus to measured EEMG). The model fitting was done using data obtained through application of the first type of stimulation pattern described above. Using a Hammerstein-type model and evaluation of the FPEC, the best model-order parameters were found to be ($l = 3$, $m = 2$). However, the FPEC values for (2,2) and (3,3) were quite close. We used two approaches for prediction of EEMG; one is based on the stimulation signal and past measured EEMG

$$\hat{x}_m(t) = \psi[s(t-1), s(t-2), \cdots, s(t-m), x(t-1), x(t-2), \cdots, x(t-l)].$$

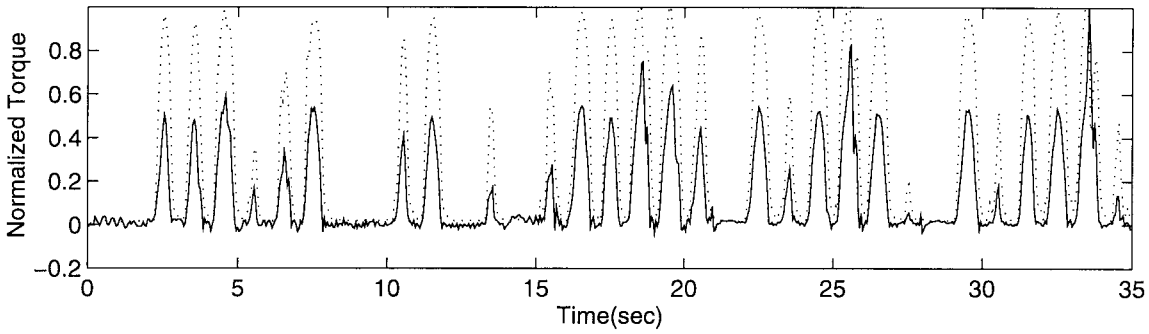

(a)

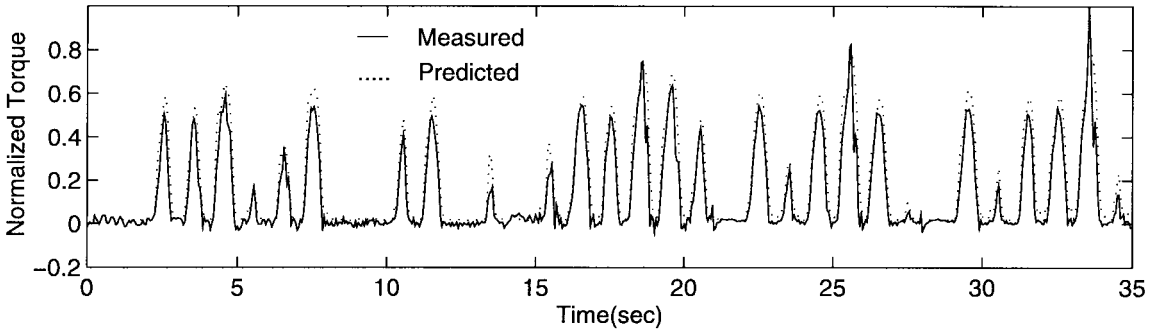

(b)

Fig. 7. The measured and predicted torque obtained using *muscle contraction dynamics model*. The model was identified during a reference day and used for prediction on different days. The prediction is based on the measured EEMG and past predicted torque $[\hat{y}_p(t)]$, for five successive 7-s trials: (a) prediction on second day *without autocalibration* and (b) prediction on second day *with autocalibration*.

TABLE III
SUMMARY OF THE RESULTS OF MUSCLE TORQUE PREDICTION ON DIFFERENT DAYS, USING A FIXED PARAMETER CONTRACTION DYNAMICS MODEL THAT HAS BEEN IDENTIFIED DURING A REFERENCE DAY. THIS REFERENCE MODEL IS THEN USED TO PREDICT THE MUSCLE TORQUE OUTPUT ON DIFFERENT DAYS, WITH AND WITHOUT AUTOCALIBRATION. THE TORQUE PREDICTION IS BASED ON THE MEASURED EEMG AND PAST PREDICTED TORQUE $(\hat{y}_p(t))$

	Subject EB					**Subject DN**				
	Reference Day	Day 2	Day 3	Day 4	Day 5	Reference Day	Day 2	Day 3	Day 4	Day 5
MSE Without Calibration	0.0504	0.2985	0.2474	0.5175	0.1461	0.0249	0.0456	0.0352	0.0470	0.0282
MSE With Calibration	0.0504	0.1146	0.0861	0.0793	0.0568	0.0249	0.0440	0.0328	0.0462	0.0261
% Reduction in MSE	0.0	61.6	65.2	84.7	61.1	0.0	3.5	6.8	1.7	7.5

The other one is based on the stimulation signal and past predicted EEMG

$$\hat{x}_p(t) = \psi[s(t-1), s(t-2), \cdots, s(t-m), \hat{x}_p(t-1), \hat{x}_p(t-2), \cdots, \hat{x}_p(t-l)].$$

Here, $s(t)$ is the stimulation input, $x(t)$ is the measured EEMG, and $\hat{x}(t)$ is the predicted EEMG. Fig. 6 is a typical example of the measured and predicted MAV of the EEMG, when both prediction approaches are used. There is very little performance difference using the two prediction approaches when identifying the excitation dynamics, as shown in Table II.

From the identified system parameters (extracted from successive trials on each of the five experiment days), the value of the steady-state gain of the excitation model (stimulus-to-EEMG) that is associated with a specific time-invariant constant pulse width stimulation signal, $\boldsymbol{S}$, can also be computed

$$\text{Gain} = \frac{X}{S} = \frac{\sum_{i=1}^{m}\sum_{j=1}^{n}\mu_{ij}[S]^{j-1}}{1-\sum_{i=1}^{l}a_i}$$

where these "a" and "μ" parameters are for the excitation model. Note that this computed steady-state gain shows significant day-to-day variation (Table II).

Using the identified *excitation model* and a knowledge of the stimulation signal for a given muscle, we can predict the

EEMG signal [$\hat{x}_p(t)$] at future times. These predicted EEMG signals can then be used in the identified contraction model, to predict the generated muscle torque. Table II summarizes the torque prediction error based on measured EEMG or predicted EEMG on each day. The most interesting result of this analysis is that the torque prediction error based on predicted EEMG is about 6% for 70 s ahead.

V. Autocalibration

One motivation for this work is the development of a method for the estimation of muscle torque that does not require a torque sensor. This is a concern in neuroprostheses development, because torque sensors are generally either unavailable or difficult to apply in a way that is consistent with clinical application. As shown above, the use of EEMG-to-torque models (rather than stimulation-to-torque models) is clearly preferable, if the EEMG measurements are available, because of the superior prediction accuracy that can be obtained.

The application of torque prediction models for controlled functional neuromuscular stimulation requires that the models work well from day to day. From the results described above, it is clear that the identified model parameters change between days. In particular, the gains of both the excitation dynamics and contraction dynamics exhibit considerable variability.

There are several possible sources for the observed day-to-day variation. Referring to Fig. 4, there may be day-to-day variations in the nonevoked components of the total neural excitation signal. Since electrode mounting and placement will differ between experimental sessions, this pathway will suffer from day-to-day variations. In addition, there will be day-to-day variations in the excitation gain, that relates neural excitation to the motor unit action potentials. Fatigue and patient's status (e.g., urinary tract infections) are factors that might cause changes in the activity of the excitation process as well as changes in the contraction process. Moreover, there are day-to-day variations in the activity of stimulated muscle due to fiber-type conversion which may occur during chronic stimulation [33]. Manifestation of fiber-type conversion appears in the EEMG as well as torque.

Compensation for EEMG Electrode Variability: In this section, we develop a method of model autocalibration that compensates for changes due to EEMG electrode variability. The procedure is as follows. During a *reference day*, the excitation model is identified, as described above, and the steady-state response to the reference input is computed. This reference gain, G_r, is identified using data that is collected when the muscle is exhibiting a constant gain, after completion of potentiation and before the onset of excitation fatigue. During subsequent operation on a different day, a new value of the stimulus-to-EEMG gain is similarly computed (from knowledge of the stimulation and the measured EEMG). Division yields a calibration factor that reflects a combination of changes in EEMG electrode pick-up properties and excitation properties; that is

$$k = \frac{G_r}{G}.$$

Although G_r and G were obtained from the identified model of the excitation process, this k factor captures changes in the relationship between the total neural signal (from all sources) and the measured EEMG.

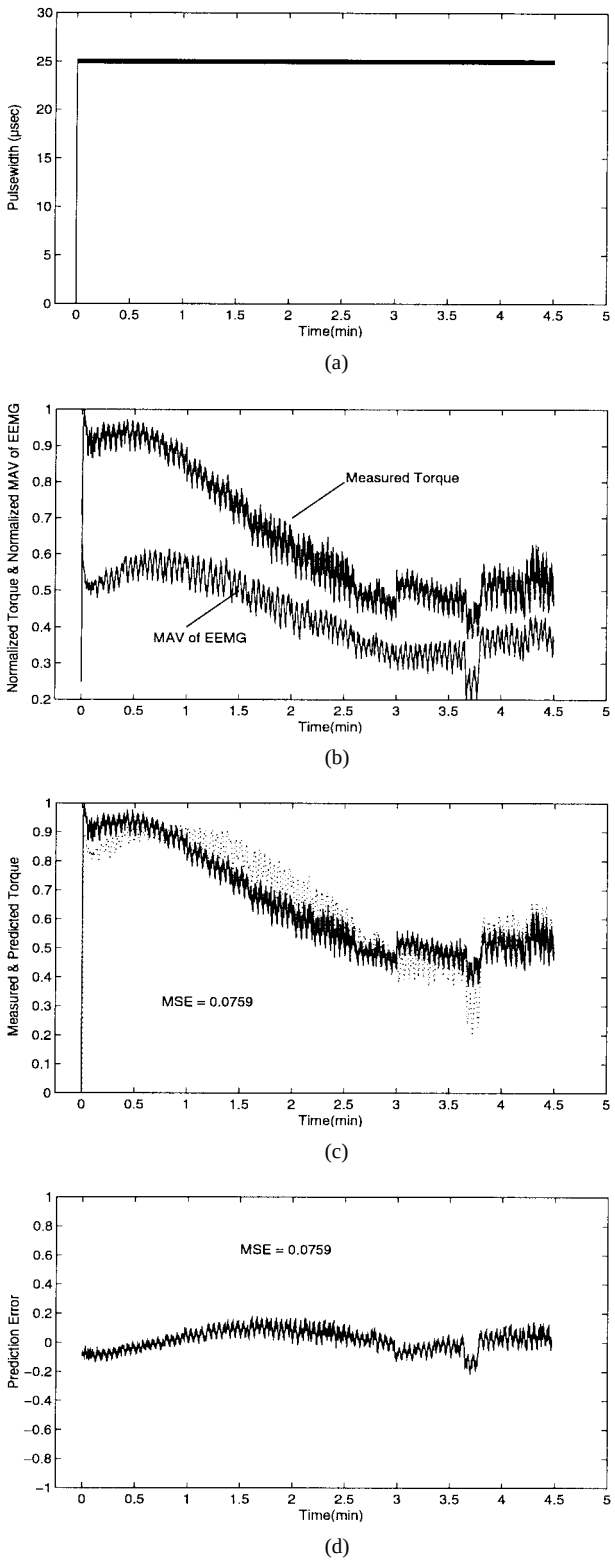

Fig. 8. (a) Five-min sustained constant pulse width input. (b) Corresponding normalized measured torque and the MAV of the normalized measured EEMG. (c) The normalized measured torque (solid line) and predicted torque (dotted line), using a fixed parameter contraction dynamics model that was identified during a previous day's experimental trial, on the same subject. (d) Prediction error. The mean-squared prediction error over the 5-min trial is about 7%.

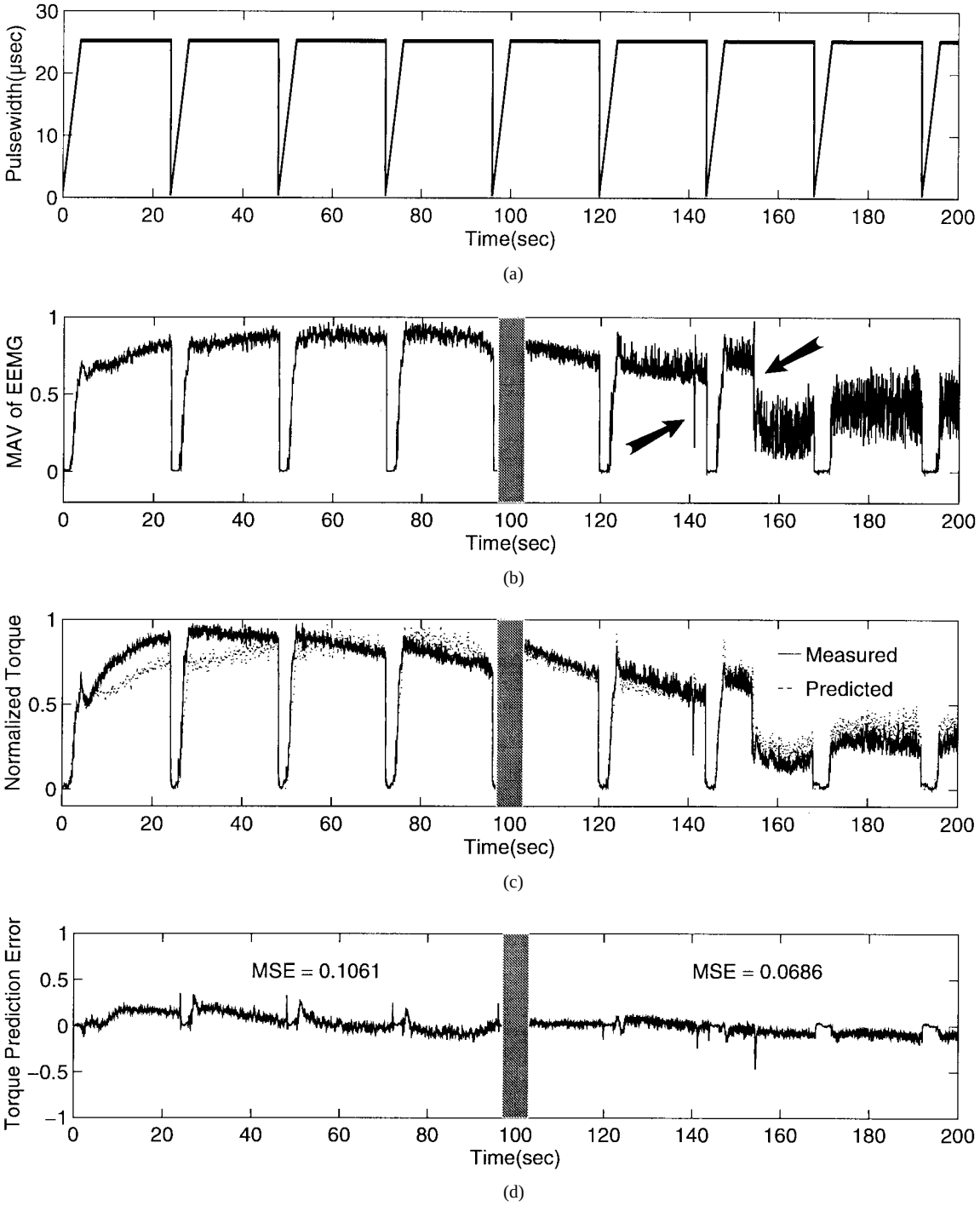

Fig. 9. (a) Portion of a 5-min input consisting of a periodic ramp-and-hold pattern. (b) Corresponding MAV of the measured EEMG. (c) The measured torque and predicted torque, using a fixed parameter contraction dynamics model that was identified during a previous day's experimental trial, on the same subject. (d) Torque prediction error.

During the reference day, an EEMG-to-torque model is also identified, using the methods described earlier. During other sessions, when torque measurements are not available, the EEMG-to-torque model that was fit during the reference day is used to predict the muscle torque, whereas the model input is multiplied by the calibration factor, k, to compensate for changes in the EEMG pickup.

The effectiveness of this calibration procedure is illustrated in Fig. 7(a) and (b), which shows the torque prediction during 35 s without calibration and with calibration, respectively. The improvement provided by this calibration is quite evident. Table III summarizes the results of muscle torque prediction on different days, using the identified model from the reference day.

VI. Potentiation and Fatigue

Using the methods described above for contraction dynamics identification, we can obtain a fixed parameter model that is capable of predicting the output torque resulting from

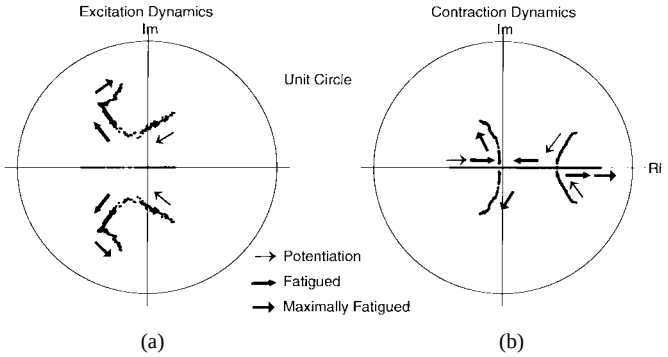

Fig. 10. The changes in the dynamics of muscle behavior due to fatigue during sustained stimulation: (a) excitation dynamics and (b) contraction dynamics. The arrows denote the direction of "movement" of the z-plane poles.

measured EEMG, despite potentiation and fatigue phenomena. This is significantly different than earlier work involving stimulation-to-torque models, where the model parameters had to be time varying [11], or where an explicit fatigue model had to be included [31].

Fig. 8 illustrates the actual measured torque and predicted torque, using a fixed parameter contraction dynamics model that was identified during a previous day's experimental trial, on the same subject. The autocalibration procedure was used. Over a period of 5 min of sustained stimulation, the torque reduction that occurs after one-half min is well tracked by the model. That is, the majority of the torque changes can be well predicted from the EEMG measurements, without adjusting the contraction dynamics model.

Fig. 9 illustrates portions of a 5-min trial. In this case, the stimulation and consequently the EEMG was varied. From time 10 to 60 s, the fixed parameter model (identified during a prior day's experiments) underestimates the output torque slightly, due to contraction potentiation. After time 160, it overestimates it slightly due to maximal contraction fatigue. However, the majority of the potentiation and fatigue response is captured by the fixed parameter contraction dynamics model. Moreover, the transient increases and decreases in torque that correspond to large changes in EEMG are very well tracked. In some instances when the stimulation rapidly increases, there is a corresponding burst of EEMG, and consequently a brief period of over-estimation of torque (at 124 s). An interesting phenomenon appears after 120 s, when the amount of oscillation of both the EEMG measurements and corresponding torque increases. At 140 s, for a very short time the neural excitation and consequently the torque, suddenly decreased for unknown reasons; however, the model follows this variation.

VII. Fatigue Dynamics

The separate identification of the excitation process and the contraction process can be used to explore the dynamics of fatigue phenomena. In particular, it is possible to relate observed changes in muscle response to changes in each of these two processes. In the model identification described in previous sections, constant parameter models were fit. In this section, we consider the identification of time-varying parameters, during intervals of sustained stimulation.

The identification of model parameters of the excitation process (i.e., stimulus as input and MAV of EEMG as output) is difficult when a constant stimulus input is used. This input does not provide a sufficiently exciting signal. However, we can fit an autoregressive model (third order) to the measured EEMG. This will allow us to obtain the poles of the excitation process system. This was done using weighted recursive least-squares methods.

Fig. 10(a) shows the movements of the z-plane poles of the resulting excitation model. The poles move during potentiation in a path that indicates increasing damping ratio and increasing natural frequency. During the onset of fatigue, the damping ratio decreases, the natural frequency increases and the oscillatory behavior of the muscle increases. However, during maximal fatigue, there is a decrease in the damping ratio and the natural frequency. The decrease in the natural frequency suggests a decrease in the firing rate. Normally, the firing rate depends on the stimulation frequency. However, when maximally fatigued, the firing rate is no longer so tightly coupled with the stimulation frequency, as shown in Fig. 11(c). The change in damping ratio corresponds to rapid system response. These results are consistent with the raw EEMG data obtained during unfatigued, fatigued, and maximally fatigued conditions, as shown in Fig. 11. Prolongation, enlargement, and decreasing the amplitude of the EEMG during fatigue is evidence of an increase in the damping ratio of the system.

Additionally, a third-order autoregressive model of the contraction dynamics was fit to the measured torque collected during sustained stimulation. Weighted recursive least-squares methods were used for model identification. This again resulted in time-varying model parameters that could be interpreted as time-varying poles, zeros, and gain of a linear system. In Fig. 10(b) the locations of these poles are indicated. The arrows denote the direction of "movement" of the z-plane poles. Note that during sustained stimulation, the oscillatory nature of the contraction dynamics initially decreases (and the pair of complex poles become real values). However, after a longer period of sustained stimulation, oscillatory response returns, at much higher frequencies. This is consistent with the overall response of the muscle during sustained stimulation, as shown earlier in Fig. 9.

VIII. Discussion

This work is concerned with developing a force-generating model of electrically stimulated muscle under isometric conditions, where the EEMG is used as the input to the model. Unlike voluntary contraction of muscle, in the electrical stimulation used here, the recruited motor units depolarize synchronously. Thus, the EEMG of the electrically stimulated muscle is the synchronous summation of the recruited motor unit action potentials. It explicitly describes motor unit recruitment and firing rate. In particular, many unpredictable disturbances of the neuromuscular system (e.g., reflex phenomena, spastic paralysis, interaction with environment, changes in stimulus

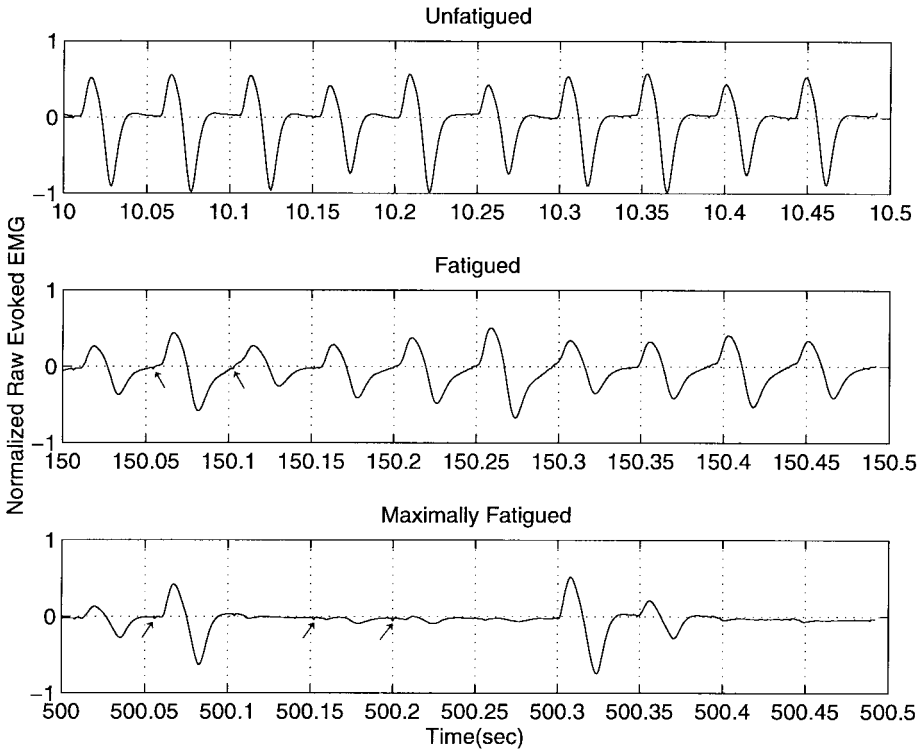

Fig. 11. One-half s of raw EEMG data obtained during unfatigued, fatigued, and maximally fatigued states.

electrode gain, F wave and H wave response, and excitation fatigue) are reflected in the EEMG signal. The use of the EEMG as a model input allows for the tracking of the torque-generation consequences of these phenomena. In this work we have demonstrated that the use of the measured EEMG as the input to a predictive model of muscle torque generation is superior to the use of electrical-stimulation signals. Although the EEMG-based method presented here captures most of variability that is manifested when the electrical stimulation signal is used, the predictability of the resulting identified model when the muscle experiences the fiber-type conversion, which occurs during chronic stimulation, should be evaluated.

The success of this approach depends upon accurate, stable, and reliable measurement of the EEMG signal. In this paper, a procedure for recording surface EMG without stimulus artifact is proposed, when the muscle is stimulated by intramuscular electrodes. The key feature of this procedure is that artifact suppression is accomplished without special filtering or switching circuitry, and that it is applicable for both real time pulse-width and stimulus-period modulation. However, the technique requires the knowledge of the approximate position of the intramuscular stimulation electrode, as well as careful placement of surface recording electrodes. Some trial and error experiments may be required in order to determine the suitable electrode size and electrode distances.

The results presented here have been verified only for isometric contractions at one joint angle. The extension of this work to non isometric conditions remains unresolved. In this work, torque prediction is provided when vastus lateralis muscle is stimulated, by activating the corresponding intramuscular electrode. However, in general, FNS will involve the contributions of several muscles to the net torque of each joint. The method proposed here must be extended for multimuscle use.

REFERENCES

[1] R. B. Stein, P. H. Peckham, and D. P. Popovic, Eds., *Neural Prostheses: Replacing Motor Function After Disease or Disability.* New York: Oxford Univ. Press, 1992.

[2] P. Crago, H. J. Chizeck, M. Neuman, and F. T. Hambrecht, "Sensors for use with functional neuromuscular stimulation," *IEEE Trans. Biomed. Eng.*, vol. BME-33, pp. 256–268, 1986.

[3] H. J. Chizeck, "Adaptive and nonlinear control methods for neural prostheses," in *Neural Prostheses: Replacing Motor Function After Disease or Disability*, R. B. Stein, P. H. Peckham, and D. P. Popovic, Eds., New York: Oxford Univ. Press, 1992, pp. 299–328.

[4] J. A. Hoffer and M. Haugland, "Signals from tactile sensors in glabrous skin suitable for restoring motor functions in paralyzed humans," in *Neural Prostheses: Replacing Motor Function After Disease or Disability*, R. B. Stein, P. H. Peckham, and D. P. Popovic, Eds. New York: Oxford Univ. Press, 1992, pp. 99–125.

[5] J. A. Hoffer, M. Haugland, and T. Li, "Obtaining skin contact force information from implanted nerve cuff recording electrodes," in *Proc. Int. Conf. IEEE/EMBS*, 1989, vol. 11, pp. 928–929.

[6] A. Szeto and R. Riso, "Sensory feedback using electrical stimulation of the tactile sense," in *Rehabilitation Engineering*, R. Smith and J. Leslie, Eds. Boca Raton, FL: CRC, 1990, pp. 29–78.

[7] D. B. Popovic, R. B. Stein, K. L. Jovanovic, R. Dai, A. Kostov, and W. W. Armstrong, "Sensory nerve recording for closed-loop control to restore motor function," *IEEE Trans. Biomed. Eng.*, vol. 40, pp. 1024–1031, Oct. 1993.

[8] M. S. Malagodi, K. W. Horch, and Schoenberg, "An intrafascicular electrode for recording of action potentials in peripheral nerves," *Ann. Biomed. Eng.*, vol. 17, pp. 397–410, 1989.

[9] N. Lang, P. E. Crago, and H. J. Chizeck, "Feedback control methods for task regulation by electrical stimulation of muscles," *IEEE Trans. Biomed. Eng.*, vol. 38, pp. 1213–1223, Dec. 1991.

[10] T. L. Chia, P. Chow, and H. J. Chizeck, "Recursive parameter identification of constrained systems: An application to electrically stimulated

muscle," *IEEE Trans. Biomed. Eng.*, vol. 38, pp. 429–442, 1991.
[11] J. Bobet, R. B. Stein, and M. N. Oguztoreli, "A linear time-varying model of force generation in skeletal muscle," *IEEE Trans. Biomed. Eng.*, vol. 40, pp. 1000–1006, 1993.
[12] D. W. Haus and R. N. Stiles, "Buckle muscle tension transducer: What does it measure?," *J. Biomech.*, vol. 22, no. 2, pp. 165–166, 1989.
[13] L. Korner, P. Parker, C. Almstrom, G. B. J. Andersson, P. Herberts, R. Kadefors, G. Palmerud, and C. Zetterberg, "Relation of intramuscular pressure to the force output and myoelectric signal of skeletal muscle," *J. Orthop. Res.*, vol. 2, no. 3, 1984.
[14] G. L. Gottlieb and G. C. Agarwal, "Dynamic relation between isometric muscle tension and the electromyogram in man," *J. Appl. Physiol.*, vol. 30, no. 3, pp. 345–351, 1971.
[15] A. L. Hof and J. Van Den Berg, "EMG to force processing I: An electrical analogue of the Hill muscle model," *J. Biomech.*, vol. 14, no. 11, pp. 747–758, 1981.
[16] S. J. Olney and D. A. Winter, "Prediction of knee and ankle moments of force in walking from EMG and kinematic data," *J. Biomech.*, vol. 18, no. 1, pp. 9–20, 1985.
[17] M. Solomonow, R. Baratta, B. H. Zhou, H. Shoji, and R. D. D'Amberosia, "The EMG-force model of electrically stimulated muscle: Dependence on control strategy and predominant fiber composition," *IEEE Trans. Biomed. Eng.*, vol. BME-34, pp. 692–703, 1987.
[18] W. K. Durfee and J. T. Dennerlein, "EMG as a feedback signal in surface FES application: Issues and preliminary results," in *Proc. Int. Conf. IEEE/EMBS*, 1989, vol. 11, pp. 1009–1010.
[19] A. Erfanian, R. M. Hashemi, and K. Badie, "An approach to modeling and controlling electrically activated paralyzed muscle using the EMG-surface response," in *Proc. IEEE Int. Conf. EMBS*, 1991, vol. 11, pp. 2329–2331.
[20] M. Solomonow, R. Baratta, T. Miwa, H. Shoji, and R. D. D'Amberosia, "A technique for recording the EMG of electrically stimulated skeletal muscle," *Orthopedics*, vol. 8, no. 4, pp. 492–495.
[21] D. Graupe, "EMG pattern analysis for patient-responsive control of FES in paraplegics for walker-supported walking," *IEEE Trans. Biomed. Eng.*, vol. 36, pp. 711–719, 1989.
[22] J. Minzly, J. Mizrahi, N. Hakim, and A. Liberson, "Stimulus artifact suppressor for EMG recording during FES by a constant-current stimulator," *Med. Biol. Eng., Comput.*, pp. 72–75, 1993.
[23] G. I. Zahalak, "An overview of muscle modeling," in *Neural Prostheses: Replacing Motor Function After Disease or Disability*, R. B. Stein, P. H. Peckham, and D. P. Popovic, Eds. New York: Oxford Univ. Press, 1992, pp. 17–57.
[24] L. A. Bernotas, P. E. Crago, and H. J. Chizeck, "A discrete-time model of electrically stimulated muscle," *IEEE Trans. Biomed. Eng.*, vol. BME-33, pp. 829–838, 1987.
[25] L. A. Bernotas, P. E. Crago, and H. J. Chizeck, "Adaptive control of electrically stimulated muscle," *IEEE Trans. Biomed. Eng.*, vol. BME-34, pp. 140–147, 1987.
[26] M. S. Hatwell, B. J. Oderkerk, C. A. Sacher, and G. F. Inbar, "The development of a model reference adaptive controller to control the knee joint of paraplegics," *IEEE Trans. Automat. Contr.*, vol. 36, no. 6, pp. 683–691, 1991.
[27] E. B. Marsolais and R. Kobetic, "Development of a practical electrical stimulation system for restoring gait in the paralyzed patient," *Clin. Orthopaed. Related Res.*, vol. 233, pp. 64–74, 1988.
[28] _____, "Implantation techniques and experiences with percutaneous intramuscular electrodes in the low extremities," *J. Rehab. Res. Develop.*, vol. 23, pp. 1–8, 1986.
[29] L. Ljung, *System Identification: Theory for the User*. Englewood Cliffs, NJ: Prentice-Hall, 1987.
[30] J. Helal and P. Bouissou, "The spatial integration effect of surface electrode detecting myoelectric signal," *IEEE Trans. Biomed. Eng.*, vol. 39, pp. 1161–1167, Nov. 1992.
[31] Y. Giat, J. Mizrahi, and M. Levy, "A musculo-tendon model of the fatigue profiles of paralyzed muscle under FES," *IEEE Trans. Biomed. Eng.*, vol. 40, pp. 664–674, July 1993.
[32] M. Knaflitz and R. Merletti, "Suppression of stimulation artifacts from myoelectric-evoked potential recording," *IEEE Trans. Biomed. Eng.*, vol. 35, pp. 758–763, Sept. 1988.
[33] D. Pette, "Skeletal muscle adaptation in response to chronic stimulation," in *Electrical Stimulation and Neuromuscular Disorders*, W. A. Nix and G. Vrbova, Eds. Berlin, Germany: Springer-Verlag, 1986, pp. 12–20.

Abbas Erfanian received the B.S. degree in computer engineering from Shiraz University, Shiraz, Iran, in 1985, the M.S. degree in computer engineering from Sharif University of Technology, Tehran, Iran, in 1989, and the Ph.D. degree in biomedical engineering from Tarbiat Modarres University, Tehran, in 1995.

From 1986 to 1988, he was an Electronics Engineer at Iran Telecommunication Research Center (ITRC), where he worked on digital in-circuit testing. From 1990 to 1992, he was an Instructor in the Computer Engineering Department at Iran University of Science and Technology, Narmak, Tehran. In 1993, he was a Visiting Research Scholar at Case Western Reserve University and VA Medical Center, Cleveland, OH, where he did research in the area of functional electrical stimulation. Since 1995, he has been an Assistant Professor of Biomedical Engineering at Iran University of Science and Technology. His research interests involve artificial neural network, biomedical signal processing, rehabilitation engineering, chaos theory and its application to biomedical problems, and functional neuromuscular stimulation. His current research projects include neuro-chaotic computing, functional neuromuscular stimulation, and state estimation of electrically stimulated muscle using EEMG.

Howard Jay Chizeck (S'74–M'79–SM'90) received the B.S. and M.S. degrees in systems and control engineering from Case Western Reserve University (CWRU), Cleveland, OH, in 1974 and 1976, respectively, and the Sc.D. degree in electrical engineering and computer science from the Massachusetts Institute of Technology, Cambridge, in 1982.

He is a Professor and Chair of the Department of Systems, Control and Industrial Engineering at CWRU, with a joint appointment in the Biomedical Engineering Department. His research interests involve nonlinear and adaptive control theory and the application of systems and control engineering to biomedical problems. His recent work has addressed control problems in the restoration of motor function by techniques of functional neuromuscular stimulation, and the automatic control of therapeutic drug delivery.

Dr. Chizeck is a Member of the IEEE Medical Technology Policy Committee and the International Federation of Automatic Control (IFAC) Technical Committee on Applications of Control to Biomedical Engineering.

Reza M. Hashemi received the B.S. degree in electrical engineering with honors from Amirkabir University of Technology, Tehran, Iran, in 1968, the M.S. degree in electrical engineering, with honors, from the University of Dayton, Dayton, OH, in 1973, and the Ph.D. degree in biomedical engineering from The Ohio State University (OSU), Columbus, in 1976.

From 1971 to 1973, he was a Teaching Assistant at the University of Dayton, and from 1973 to 1976 he was a Research Associate at OSU. After completing a post doctoral fellowship at OSU in 1977, he joined Amirkabir University of Technology where he is now Professor of Electrical Engineering. He is the founder of the Biomedical Engineering Department at the same university. His research interest include feedback control systems, digital control systems, state variable methods in control systems, analysis of nonlinear systems, optimal and adaptive control theory, biomedical instrumentation, biological system modeling, biological signal processing, neuromuscular control systems, cybernetic prostheses, rehabilitation engineering, and chaos and its applications to biomedical engineering.

Dr. Hashemi received the "khwarazmi" Scientific highest distinction award for conducting the Tehran Cybernetic Arm Research Team in 1990. He is a member of the New York Academy of Science and the Iranian Academy of Science, a member of the Iranian National Standard Council, and member and Vice Director of the Iranian National Scientific Research Council.